Kinetics and Thermodynamic Study for Adsorption of Methylene Blue onto Mulberry Tree (Morus nigra L) Roots Powder

Mansour Faraj[a] and *Mohamed Erhayem[a] and Ragwan Mohamed[b]

[a] Chemistry Department, Faculty of Science, Sebha University, Libya

[b] Chemistry Department, Faculty of Science, Sitre University, Libya

*Corresponding author: moh.erhayem@sebhau.edu.ly

Abstract In this research, the batch adsorption models were conducted for the adsorption of Methylene Blue (MB) onto grounded Morus Nigra L roots powder (MNLRP) surface. Different adsorption parameters were applied in order to study the adsorption processes at 25, 35 and 45°C. Adsorption kinetics data were modeled with different kinetic models and the results revealed that the pseudo-second order model was the best fitting model. The results from thermodynamic parameters showed that the adsorption process was spontaneous and endothermic processes. The parameters values of standard free energy (ΔG^0) were -1.730, -2.124 and -2.234 KJ/mol at 25, 35 and 45°C, respectively. The values of change standard enthalpy (ΔH^0) is 12.6 KJ/mol and the values of change standard entropy (ΔS^0) is 59.4 J/mol K. The randomness was increased at the solid/liquid interface. The findings in this study that the MNLRP could be used to remove MB dyes from aqueous solutions.

Keywords: kinetic, Methylene Blue, Mulberry tree roots, Thermodynamic.

دراسة حركية وترموديناميكية لامتزاز صبغة الميثيلين الأزرق على مسحوق جذور شجر التوت

منصور فرج[a] و *محمد أرحيم[a] و رجوان محمد[b]

[a] قسم الكيمياء–كلية العلوم–جامعة سبها، ليبيا

[b] قسم الكيمياء–كلية العلوم–جامعة سرت، ليبيا

*للمراسلة: moh.erhayem@sebhau.edu.ly

الملخص في هذا البحث، تم اجراء نماذج الامتزاز لامتزاز صبغة الميثيلين الأزرق على سطح مسحوق جذور التوت. قياسات مختلفة تم تطبيقها لدراسة عمليات الامتزاز عند 25م°، 35م°، و45م° . بيانات حركية الامتزاز تم تمثيلها مع نماذج الحركية المختلفة وأظهرت النتائج ان نموذج الرتبة الثانية هو النموذج المناسب لعملية الامتزاز . نتائج قياسات الثرموديناميك اظرت ان عملية الامتزاز عملية تلقائية وماصة للحرارة حيث كانت قيم التغير في طاقة الحرة القياسية (ΔG^0) 1.730–، 2.124–، 2.234– كيلوجول/مول عند 25م°، 35م°، و45م° على التوالي وقيمة التغير في المحتوى الحراري (ΔH^0)12.6 كيلوجول/مول. قيمة التغير في عشوائية النظام القياسية (ΔS^0)59.4 جول/مول وهي تشير زيادة التداخل صلب/سائل. وجدنا من هذه الدراسة ان مسحوق جذور التوت يمكن استخدامها لإزالة صبغة الميثيلين الأزرق من المحلول المائي.

الكلمات المفتاحية: الحركية، الميثيلين الأزرق، جذور شجر التوت، الترموديناميك.

1. Introduction:

pollution is becoming a big environmental problem and a serious concern for researchers. It is found in several forms such as water pollution, air pollution, soil pollution, Noise Pollution and Radioactive pollution etc [1-3]. Walker et al (2019) said, water pollution is mow a sensitive topic due to water is important for the life [4].

dyes are considered as one of the most dangerous pollutants to hydrosphere. Dyes have been widely employed in paper, textile, paper, rubber, plastics, leather, cosmetics, pharmaceutical and food industries. The released wastewater containing dyes into ecosystems could be affected on humans. Noorimotlagh et al (2019)

mentioned that the existence of 1 mg/L of dye in water can cause skin irritation, dermatitis, allergy and provoke carcinogenic and even mutagenic effects in aquatic organisms and humans [5]. Therefore, the way to remove those dyes from wastewater is still desirable.

Adsorption is one of the most economically methods comparing to other removal techniques used in these days, which uses to remove pollutants like dyes from the hydrosphere [6]. Many studies have earlier been conducted on using waste materials to remove dyes as adsorbent including agricultural wastes such as biochar [7], Orange peel [8] rice husk [9], Straw [10], almond shell [11],

Pomelo peel **[12].** However, in our previous research, Mulberry tree roots powder (MNLRP) was used as a sorbent to remove methylene blue from aqueous solution **[13]**. In this research, the adsorption kinetic models such as Pseudo-First order model, Pseudo-Second order model and Intraparticle Diffusion model, were calculated. The thermodynamic parameters such as the change standard Gibbs free energy (ΔG^0) and change standard enthalpy (ΔH^0), change standard entropy (ΔS^0) and activation energy (E_a) were also determined.

2. Materials and Methods

2.1. Chemicals and Instruments

The Methylene blue dye used in this study was purchased from DPH company. The instruments which used in this study: UV-Vis spectrophotometer (Jenway model 6305), FTIR spectrophotometer 360 Thermo, and mechanical shaker equipped with a thermostatic water (Clifton).

2.2. Adsorbent Preparation

The Morus nigra L roots (MNLR) were collected from Samno Village, Albowanise State, north of Sebha City, Libya. The collected MNLR were washed with distilled water for several times and were kept on dry place under 25°C. The dry roots were then grounded with grinder and sieved using different sieves at 0.250 mm. The MNLRP was stored in an air-tight plastic container for all further experiments throughout this work.

2.3. Preparation of Standard Solutions

Stock standard solution of MB with a concentration of 500 mg/L was prepared by dissolving a certain weight of MB in deionized water and kept in refrigerator for further experiments. The desired MB concentrations were prepared from dilution of the stock solution of MB solution for each sorption experiment.

2.4 Adsorption experiment

The equilibrium concentration of MB after adsorption on MNL determined using UV-Vis spectrophotometer at 660 nm after 120 min shacking. Standard curves were evaluated and used in order to determine the concentration of MB at each experiment. The calibration curves were conducted in the range 1-8 mg/L.

2.4. Adsorption Kinetic Experiments

100 mg MNLRP was added to 15 ml of 80 mg/L MB and then agitated at 400 rpm for contact times ranging from 15 min to 135 min at different temperature of 25, 35 and 45°C. Then, the concentrations of filtrated MB left in solution was measured by the absorption at 660 nm.

2.5. Adsorption thermodynamic experiments

100 mg MNLRP was added to 15 mL of 40, 50, 70, 90, 120 mg/L MB at different temperature (25, 35 and 45°C). The mixture was stirred at 400 rpm for 60 min. Then, the concentration of filtrated MB left in solution measured by the absorption of each solution at 660 nm using UV-Vis spectrophotometer.

2.6. Mathematical adsorption calculations

The adsorption capacity of the amount MB dye adsorbed onto MNLRP surface was calculated using the following equation:

$$q_t = \frac{C_0 - C_t}{m_S} \times V \tag{1}$$

$$q_e = \frac{C_0 - C_e}{m_S} \times V \tag{2}$$

Where: C_0 and C_e (mg/L): the initial and the final concentrations of adsorbate in flasks, respectively; C_t (mg/L): the concentrations of adsorbates at time t. V: the volume of the solution (L) and m_s: the mass of dry adsorbent used (g) **[14]**. Adsorption Kinetic Models of the adsorption MB-MNLRP were evaluated using pseudo-first order, pseudo-second order, intraparticle diffusion. Pseudo first-order, Pseudo second-order and Intraparticle diffusion kinetic models can be written as equation 3, 4, 6 respectively:

$$ln\left(q_e - q_t\right) = ln\, q_e - k_1 t \tag{3}$$

$$\frac{t}{q_t} = \frac{1}{k_2 q_e^2} + \frac{1}{q_e} t \tag{4}$$

$$k_2 q_e^2 = h = \frac{1}{intercept} \qquad \left(at\ t = 0\right) \tag{5}$$

$$q_t = k_d t^{1/2} + C \tag{6}$$

Where: q_e and q_t are the amounts of MB (mg/g) at equilibrium and at time t, respectively. k_1 is the pseudo-first order equilibrium rate constant (min^{-1}). The values of q_e and k_1 were determined from the linear plot of $ln(q_e - q_t)$ against t, (ln q_e = intercept) and (k_1=slope). The expression in equation (h) denotes the initial sorption rate (mg/g min) at t=0. q_e and k_2 is the equilibrium rate constant of pseudo-second order adsorption (g/mg min). q_e, k_2 and h can be determined from the slope and intercept of the straight lines in plot of t/q_t versus t. Intraparticle diffusion model used to identify the diffusion mechanisms (internal surface and pore diffusion). The intra-particle diffusion is a function of $t^{1/2}$ and can be defined by Equation (6), C (mg/g) is the intercept and k_d (mg/g.min$^{1/2}$) is the intraparticle diffusion rate constant (slope) **[15]**. Thermodynamic parameters such as the change in standard free energy (ΔG^0), enthalpy (ΔH^0), and entropy (ΔS^0) were calculated using the Van't Hoff equation by the following equations:

$$\ln K_0 = \frac{-\Delta H^0}{RT} + \frac{\Delta S^0}{R}$$

(7)

$$\Delta G^0 = -RT \ln K_0$$

(8)

Where: intercept of $\ln q_e$ vs C_e plot to obtain ΔG^0, the change in ΔH^0 and ΔS^0 are calculated from the slope and intercept of plot $\ln K_0$ versus $1/T$ respectively, K_0 is thermodynamic equilibrium constant it can be calculated through the following equation:

$$K_S = \frac{q_e}{C_e} \times \frac{v_1}{v_2}$$

(9)

Where: v_1 is the activity coefficient of the adsorbed solute, and v_2 is the activity coefficient of the solute in equilibrium suspension, when equilibrium concentration approaching to zero the ratio tends to unity as follows:

$$\lim_{C_e \to 0} \ln \frac{q_e}{C_e} = K_0$$

(10)

Representationally, $\ln q_e/C_e$ vs C_e can be account K_0 from the intercept[1].

The activation energy, E_a of adsorption was also calculated from the linearized Arrhenius equation

$$\ln k_2 = \ln K_0 - \frac{E_a}{RT}$$

(11)

Where: k_2 is the rate constant second-order of adsorption (g/mol min), K_0 is the independent temperature factor (g/mol min), E_a is the activation energy of adsorption ($KJ mol^{-1}$), R is the gas constant ($J mol^{-1}K^{-1}$) and T is the solution temperature (K). A plot of $\ln k_2$ vs $1/T$ gives a straight line, and the corresponding activation energy was determined from the slope of the linear plot.

2.7. Statistical Methods

Coefficient of determination (R^2), Chi-squared test (χ^2), Sum of the Squares of the Errors (SSE), Hybrid fractional error function (HYBRID), Marquardt's Percent Standard Deviation (MPSD) were used for interpretation of results process as the following equations:

$$\chi^2 = \sum_{i=1}^{n} \frac{(q_{e,\exp} - q_{e,calc})^2}{q_{e,calc}}$$

(12)

$$SSE = \sum_{i=1}^{n} (q_{e,calc} - q_{e,\exp})^2$$

(13)

$$HYBRID = \frac{100}{n-p} \sum_{i=1}^{n} \frac{(q_{e,\exp} - q_{e,calc})^2}{q_{e,\exp}}$$

(14)

$$MPSD = 100 \times \sqrt{\frac{1}{n-p} \sum_{i=1}^{n} \left[\frac{(q_{e,\exp} - q_{e,calc})}{q_{e,\exp}} \right]^2}$$

(15)

Where: $q_{e,cal}$ is the equilibrium capacity obtained from the adsorption model (mg / g) and $q_{e,exp}$ is then equilibrium capacity (mg / g) from the experimental data n is the number of data points, and p is the number of parameters in isotherm equations and kinetic equations[16].

3. Results and Discussion

3.1. Characterization of MNLRP surface

Figure 1 shows the FT-IR spectra for MNLRP before and after adsorption of MB. The spectrum showed the functional groups on the surface of MNLRP, which represent adsorption sites on MNLRP surface. The function groups on MNLRP surface was noted a stretching of the O-H or N-H group at the range 3200-3500 cm-1, CH group at 2800-3000 cm-1, stretching C=O at 1700-1600cm-1, stretching C-C between 1400-1500 and stretching C-O at 1050-1260cm-1. Also, it was noted that the spectrum shows the bonds before and after adsorption process and the spectra of before and after adsorption are very close in wavenumber, nut not in the intensities. This indicates that there are no chemical bonds between MB and MNLRP, therefore, the adsorption of MB on MNLRP could be physisorption. Rahim et al 2016 was found the similar behavior on his research [17].
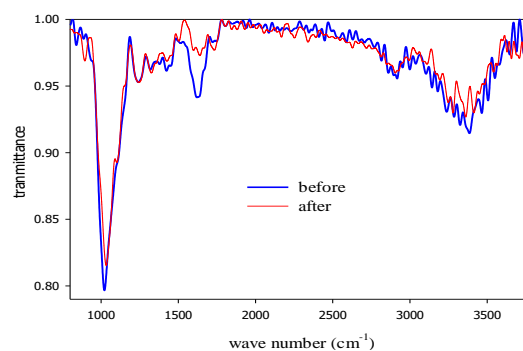
Figure 1. FTIR spectra for MNLRP before and after adsorption process

3.1. Adsorption kinetic studies

The adsorption kinetic models for the interaction between MB and MNLRP surface were investigated at different time, t and temperature, T. The results obtained are listed in **Table 1.** Three models had been studied to investigate the adsorption kinetics such as Pseudo-first order, Pseudo-second order and intra-particle diffusion. However, the statistical analysis of R^2, χ^2 , HYBRID and MPSD were also studied.

In the case of the pseudo-first order model, it was found that the value was low. Therefore,

pseudo-first order model cannot explain the kinetics of the interaction MB-MNLRP as shown in Figure 2. In the other case, the intraparticle diffusion model was used to explain the adsorption kinetics as well. It was appeared that the plots do not pass through the origin, therefore, the intraparticle diffusion is not the only rate limiting step, the intercept in this model gives information about the thickness of the boundary layer (amount of MB, in milligrams, adsorbed per gram of MNLRP) shown in Figure 4. On the other case, Pseudo-second order model was used to illustrate the adsorption kinetics. It was became clear that the interaction between MB and MNLRP surface belongs to pseudo-second order model based on the results from R^2, χ^2, HYBRID and MPSD as listed in Table 1. The value for this model is 0.9999 at 25, 35 and 45 °C. Therefore, kinetic adsorption processes of MB onto MNLRP surface depends on the both of concentration of MB and MNLRP. Similar results were reported on other researches **[15, 18, 19]**
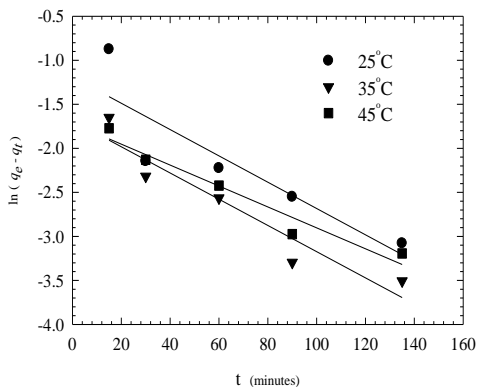
Figure 2. relationship of the kinetics data by First-order model under conditionsCo80mg/L, 400rpm, dosage 0.1g, 15mL, pH=7, 298,308 and 318
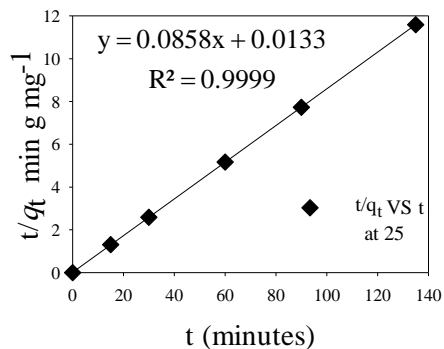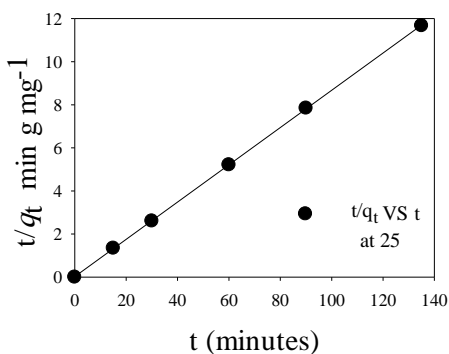
Figure 3. relationship of the kinetics data by second-order model under conditions Co 80 mg/L,400rpm, dosage 0.1g, pH=7
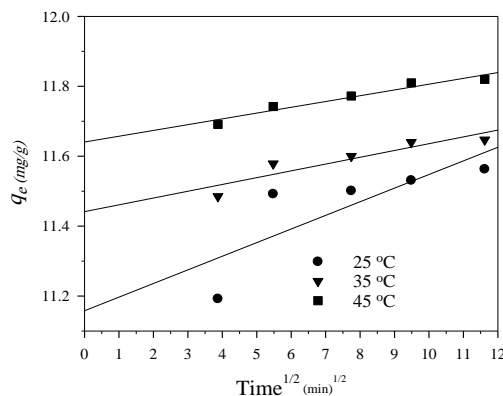
Figure 4. relationship of the kinetics data by Intraparticle diffusion model under conditions Co 80 mg/L, 400rpm, dosage 0.1g, 15mL, pH=7, 298,308 and 318K.

Table 1. The adsorption kinetic parameters for adsorption of MB on MNLRP at different temperatures, 400rpm,80mg/L, 0.1g, 15mL, pH=7

Temperatures (K)	298K	308K	318K
$q_{e, \, exp \, (mg/g)l}$ after 4 hours	11.609	11.677	11.861
Pseudo-First order model			
$q_{e, \, cal(mg/g)l}$	0.3045	0.1857	0.1801
$K_1(min^{-1})$	0.0149	0.0149	0.0119
R^2	0.780	0.9072	0.9493
χ^2	419.7	711.1	757.6
SSE	127.8	132.0	136.4
HYBRID	220.2	226.2	230.1

MPSD	56.22	56.82	57.29
$q_{e,\ cal(mg/g)l}$	**11.**561	11.655	11.820
h mg g^{-1} min^{-1}	41.494	75.188	80.645
k$_2$ g mg^{-1} min^{-1}	0.3100	0.5510	0.5770
R^2	0.9999	0.9999	0.9999
χ^2	0.00019	0.00004	0.00014
SSE	0.0023	0.00048	0.0017
HYBRID	0.0039	0.0008	0.0028
MPSD	0.2387	0.1087	0.1996
Intraparticle diffusion model			
(K_d)	0.039	0.0194	0.0166
C (mg/g)	11.158	11.442	11.641
R^2	0.6426	0.846	0.9426

3.2.   Thermodynamic study

Thermodynamic parameters was determined using the equations 7 and 8 and plotted as shown in Figure 6 and listed in Table 2. The values of ΔG are to be -1.730, -2.124 and -2.234 KJ/mol at 25, 35 and 45°C, respectively, This indicates that the interaction occurs spontaneous and becoming more spontaneous with increasing temperature. Also, the ΔH and ΔS values are to be 12.61 KJ/mol and 59.35 J/(mol.K), respectively as listed in Table 2. The positive value of means that the adsorption of MB on MNLRP is endothermic processes. This explains the increase in removal percentage and adsorption efficiency with increased temperature. The positive value of ΔS means that the adsorption of MB on MNLRP is irreversible and the adsorption process is accompanied increase in entropy **[20].**
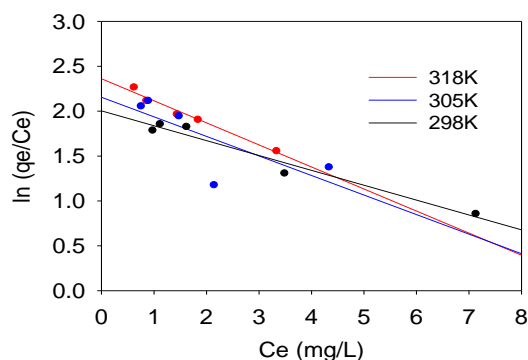
Figure 5. Thermodynamic equilibrium constant at different temperature**.**
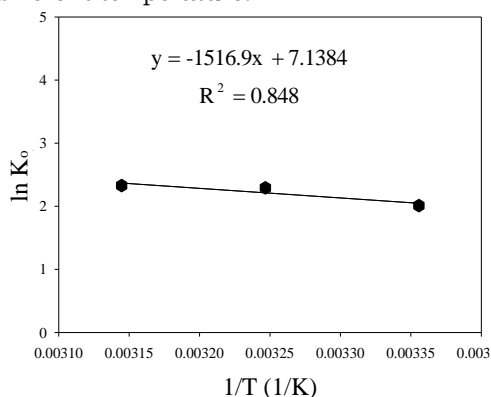
Figure 6. Plots of ln Ko vs 1/T for the Van't Hoff equation

The activation energy was calculated from the slope of plot lnk$_2$ vs. 1/T, as shown in **Figure** 7. The value of   is to be 24.75 KJ/mol. This is confirmed that the adsorption process of MB onto MNLRP is physical adsorption process due to the physical adsorption the activation energy value is lower   than   40   kJ/mol**[21,22].**
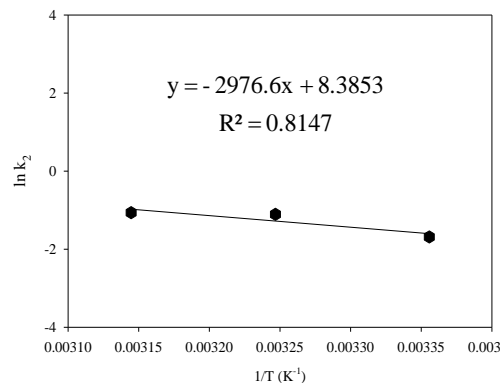
Figure 7. Plots of ln k2 vs 1/T for the Arrhenius.

Table 2. Thermodynamic parameters for adsorption of MB on MNLRP

Temp K	K_0 L/g	ΔG^0 KJ/mol	ΔH^0 KJ/mol	ΔS^0 J/mol.K	E_a KJ/mol
298K	2.010	-1.730	12.61	59.35	24.75
308K	2.291	-2.124			
318K	2.327	-2.234			

4. Conclusion

The kinetic study adsorption of MB on MNLRP indicated that interaction belonged to pseudo-second order model. The activation energy for adsorption of MB on MNLRP and FTIR spectra for MNLRP before and after adsorption process indicated that the adsorption was physisorption. Adsorption of MB on MNLRP was spontaneous, endothermic and increased randomness at the solid/liquid interface. Therefore, MNLRP could be used as adsorbent to remove MB from aqueous solutions.

5. References

[1]- AkankshaKalra, H.P., et al., Adsorption of Dyes from Water on to Bamboo-Based Activated Carbon-Error Analysis Method for Accurate Isotherm Parameter Determination. 2019. **1**(1): p. 1-11.

[2]- Soberanes, S., et al., Metformin targets mitochondrial electron transport to reduce air-pollution-induced thrombosis. 2019. **29**(2): p. 335-347. e5.

[3]- Oguntunde, P., et al., A Study of Noise Pollution Measurements and Possible Effects on Public Health in Ota Metropolis, Nigeria. Open Access Maced J Med Sci. 2019 Apr 30; 7 (8): 1391-1395. 2019.

[4]- Walker, D., et al., Surface water pollution, in Environmental and Pollution Science. 2019, Elsevier. p. 261-292.

[5]- Noorimotlagh, Z., et al., Adsorption of textile dye in activated carbons prepared from DVD and CD wastes modified with multi-wall carbon nanotubes: Equilibrium isotherms, kinetics and thermodynamic study. 2019. **141**: p. 290-301.

[6]- Mohamed, E.F., Removal of organic compounds from water by adsorption and photocatalytic oxidation. 2011.

[7]- de Jesus, J., et al., Adsorption of aromatic compounds by biochar: influence of the type of tropical biomass precursor. 2019. **26**(7): p. 4291-4299.

[8]- Arami, M., et al., Removal of dyes from colored textile wastewater by orange peel adsorbent: equilibrium and kinetic studies. 2005. **288**(2): p. 371-376.

[9]- Rachna, K., A. Agarwal, and N.J.M.T.P. Singh, Rice husk and Sodium hydroxide activated Rice husk for removal of Reactive yellow dye from water. 2019. **12**: p. 573-580.

[10]- Yang, S.-S., et al., Generation of high-efficient biochar for dye adsorption using frass of yellow mealworms (larvae of Tenebrio molitor Linnaeus) fed with wheat straw for insect biomass production. 2019. **227**: p. 33-47.

[11]- İzgi, M.S., et al., Preparation and Characterization of Activated Carbon from Microwave and Conventional Heated Almond Shells Using Phosphoric Acid Activation. 2019. **52**(5): p. 772-789.

[12]- Zhang, B., et al., Removal of methyl orange dye using activated biochar derived from pomelo peel wastes: performance, isotherm, and kinetic studies. 2019: p. 1-12.

[13]- Faraj, M. and M. Erhayem, Langmuir, Freundlich, Temkin and Dubinin–Radushkevich isotherm studies of equilibrium sorption of Methylene Blue from Aqueous Solution onto Mulberry tree (Morus nigra L) roots powder. Journal of Pure Applied Sciences, 2018. **17**: p. 100-107.

[14]- Wang, F.Y., H. Wang, and J.W. Ma, Adsorption of cadmium (II) ions from aqueous solution by a new low-cost adsorbent—Bamboo charcoal. Journal of hazardous materials, 2010. **177**(1-3): p. 300-306.

[15]- Bouhamed, F., Z. Elouear, and J. Bouzid, Adsorptive removal of copper (II) from aqueous solutions on activated carbon prepared from Tunisian date stones: equilibrium, kinetics and thermodynamics. Journal of the Taiwan Institute of Chemical Engineers, 2012. **43**(5): p. 741-749.

[16]- Chowdhury, S. and P. Saha, Adsorption Kinetic Modeling of Safranin onto Rice Husk Biomatrix Using Pseudo-first-and Pseudo-second-order Kinetic Models: Comparison of Linear and Non-linear Methods. Clean–Soil, Air, Water, 2011. **39**(3): p. 274-282.

[17]- Rahim, A.A. and Z.N. Garba, Efficient adsorption of 4-chloroguiacol from aqueous solution using optimal activated carbon: Equilibrium isotherms and kinetics modeling. Journal of the Association of Arab Universities for Basic and Applied Sciences, 2016. **21**: p. 17-23.

[18]- Bharathi, K. and S. Ramesh, Removal of dyes using agricultural waste as low-cost adsorbents: a review. Applied Water Science, 2013. **3**(4): p. 773-790.

[19]- Gonte, R. and K. Balasubramanian, Heavy and toxic metal uptake by mesoporous hypercrosslinked SMA beads: isotherms and kinetics. Journal of Saudi Chemical Society, 2016. **20**: p. S579-S590.

[20]- Donat, R., et al., Thermodynamics of Pb2+ and Ni2+ adsorption onto natural bentonite from aqueous solutions. Journal of colloid and interface science, 2005. **286**(1): p. 43-52.

[21]- Banerjee, S. and M. Chattopadhyaya, Adsorption characteristics for the removal of a toxic dye, tartrazine from aqueous solutions by a low cost agricultural by-product. Arabian Journal of Chemistry, 2017. **10**: p. S1629-S1638.

[22]- Inglezakis, V.J. and A.A. Zorpas, Heat of adsorption, adsorption energy and activation energy in adsorption and ion exchange systems. Desalination and Water Treatment, 2012. **39**(1-3): p. 149-157.